

ABSTRACT

JONES, RANDY EARL. Feedback Design Prescription for the Attitude Control of Unmanned Rockets. (Under the direction of Charles Hall)

In the case of a rocket in need of a system of attitude control, there was a desire to develop a routine process of feedback controller design. In this process of controller design, a rocket of known properties and a chosen flight plan were used in conjunction with formulated equations of motion to choose appropriate control gains. Simulink was used to model and verify the chosen controller design.

For the system and control gain values were chosen, the maneuvers of the flight plan was initially unachievable by the control system when modeled in Simulink. To improve the system, the initial control gains were reduced and the stepped commands were replaced with ramped commands. With these changes, the rocket is expected to be capable of achieving the chosen flight plan, completing the control system design prescription.

Although a control system was chosen, improvements can still be made. Alternative controller designs were suggested for further study in an attempt to improve upon the proportional feedback system presented in this work. A PID control system was particularly recommended for steady-state error improvement. In addition, a preliminary test launch with the chosen control system and gyros was suggested for data recording. The recorded data could be compared to the simulation for refinement of the control system and its control gains.

Proportional Feedback Design for Attitude Control of Unmanned Rockets

by
Randy Earl Jones

A dissertation submitted to the Graduate Faculty of
North Carolina State University
in partial fulfillment of the
requirements for the Degree of
Master of Science

Aerospace Engineering

Raleigh, North Carolina

2018

APPROVED BY:

Andre Mazzoleni

Matthew Bryant

Charles Hall
Chair of Advisory Committee

BIOGRAPHY

Randy Earl Jones II was born January 14, 1991 in La Mesa, California. With his family, he found his roots in North Carolina where he spent the majority of his life thus far. After his passion for science and its applications was realized, he graduated from North Carolina State University with a Bachelor of Science Degree in Aerospace Engineering in May of 2016. Without pause in his academic career, he continued onward at his alma mater to pursue a Master of Science Degree in Aerospace Engineering.

TABLE OF CONTENTS

LIST OF TABLES.....	v
LIST OF FIGURES	vi
LIST OF SYMBOLS	vii
1. INTRODUCTION	1
1.1. Objective of the Present Work.....	1
1.2. Control System Design Approach	1
2. ROCKET DESIGN	3
3. FLIGHT PLAN.....	5
4. DYNAMICS ANALYSIS	8
4.1. Coordinate Systems.....	8
4.2. Equations of Motion	9
4.3. Roll Dynamics	10
4.4. Pitch Dynamics	12
5. GAIN SCHEDULE DETERMINATION	14
5.1. Roll Control Gain Determination.....	14
5.2. Pitch Control Gain Determination	18
6. RESULTS AND DISCUSSIONS.....	21
6.1. Roll Control Results.....	22
6.2. Modifying Roll Gain Values to Improve System Response	23
6.3. Modifying the Roll Command to Improve System Response.....	24
6.4. Pitch Control Results	26
7. CONCLUSIONS AND RECOMMENDATIONS	28
7.1. Conclusions of the present work	28
7.2. Recommendations for Further Study.....	29
8. REFERENCES	31
9. APPENDICES.....	32

Appendix A - Vertical Flight Simulation Program for MATLAB	33
Appendix B - Fourth-Order Runge-Kutta Integrator for MATLAB	34
Appendix C - Rocket Vertical Flight State Equation Program for MATLAB	35
Appendix D - Transfer Function Input Program for MATLAB and Simulink	36

LIST OF TABLES

Table 1.1 - Control System Plan of Design.....	1
Table 2.1 - Relevant Rocket Properties	3
Table 2.2 - Relevant Rocket Coefficients.....	4
Table 3.1 - Flight Plan at Discrete Times	7
Table 6.1 - Selected Control Gain Values.....	21
Table 7.1 - Proposed Flight Plan.....	28
Table 7.2 - Proposed Gain Schedule	29

LIST OF FIGURES

Figure 3.1 - Expected Rocket Flight.....	6
Figure 4.1 - Rocket Frame and Relevant Angles	8
Figure 4.2 - Rocket Axes and Attitude Angles	10
Figure 4.3 - Roll Control Feedback Loop	11
Figure 4.4 - Pitch Control Feedback Loop	12
Figure 5.1 - Root Locus Plot of Roll Dynamics, 3.0 Seconds into Flight	14
Figure 5.2 - Root Locus Plot of Roll Dynamics with Lead Circuit.....	15
Figure 5.3 - System Response to a 90 Degree Step Input	16
Figure 5.4 - System Response with Various Gain Values	17
Figure 5.5 - System Roll Response at Various Velocities	18
Figure 5.6 - Root Locus Plot of Pitch Dynamics with Lead Circuit	19
Figure 5.7 - System Response at Various Velocities to a 10 Degree Step Input, $K_p = 2.2$	20
Figure 6.1 - Simulink Roll Maneuver Simulation.....	22
Figure 6.2 - System Response to Modified Gain Schedules.....	23
Figure 6.3 - Ramped Command System Responses	24
Figure 6.4 - System Response to Gain Change and Ramped Command	25
Figure 6.5 - Simulink Pitch Maneuver Simulation	26
Figure 6.6 - Ramped Pitch Maneuver Simulation.....	27

LIST OF SYMBOLS

Roman Symbols

C_{Fx}	Non-dimensionalized x-directional force coefficient
C_{Fy}	Non-dimensionalized y-directional force coefficient
C_{Fz}	Non-dimensionalized z-directional force coefficient
C_l	Non-dimensionalized rolling moment coefficient
C_{lp}	Rolling moment coefficient due to roll rate
C_{lr}	Rolling moment coefficient due to yaw rate
$C_{l\beta}$	Rolling moment coefficient due to sideslip angle
$C_{l\delta}$	Rolling moment coefficient due to flap angle
C_m	Non-dimensionalized pitching moment coefficient
C_{mq}	Pitching moment coefficient due to pitch rate
C_{mu}	Pitching moment coefficient due to flight velocity
$C_{m\alpha}$	Pitching moment coefficient due to attack angle
$C_{m\dot{\alpha}}$	Pitching moment coefficient due to attack rate
$C_{m\delta}$	Pitching moment coefficient due to flap angle
C_n	Non-dimensionalized yawing moment coefficient
C_{np}	Yawing moment coefficient due to roll rate
C_{nr}	Yawing moment coefficient due to yaw rate
$C_{n\beta}$	Yawing moment coefficient due to sideslip angle
C_w	Non-dimensionalized weight coefficient
C_{xq}	X-directional force coefficient due to pitch rate
C_{xu}	X-directional force coefficient due to flight velocity
$C_{x\alpha}$	X-directional force coefficient due to attack angle
$C_{x\dot{\alpha}}$	X-directional force coefficient due to attack rate
$C_{x\delta}$	X-directional force coefficient due to flap angle
C_{yp}	Y-directional force coefficient due to roll rate

C_{yr}	Y-directional force coefficient due to yaw rate
$C_{y\beta}$	Y-directional force coefficient due to sideslip angle
$C_{y\phi}$	Y-directional force coefficient due to attack angle
$C_{y\psi}$	Y-directional force coefficient due to yaw rate
$C_{y\delta}$	Y-directional force coefficient due to flap angle
C_{zq}	Z-directional force coefficient due to pitch rate
C_{zu}	Z-directional force coefficient due to flight velocity
$C_{z\alpha}$	Z-directional force coefficient due to attack angle
$C_{z\dot{\alpha}}$	Z-directional force coefficient due to attack rate
$C_{z\delta}$	Z-directional force coefficient due to flap angle
d	Reference length, rocket diameter
I	Moment of inertia
k	Gain
l	Reference length from CG to point of thrust
L	Rolling moment
m	Mass
M	Pitching moment
N	Yawing moment
p	Roll rate
q	Pitch rate
\bar{q}	Dynamic pressure
r	Yaw rate
s	Laplace variable
S	Reference area
U	Flight velocity

Greek Symbols

α	Attack angle
----------	--------------

β	Sideslip angle
Δ	Change in
δ_ϕ	Pitch flap deflection angle
δ_θ	Roll flap deflection angle
θ	Pitch angle
θ_0	Initial pitch angle
ϕ	Roll angle
ψ	Yaw angle
γ	Flight path angle

Subscripts

comm	commanded control angle
E	Earth reference frame
R	Rocket reference frame
x	x-direction
xx	x-plane
xz	xz-plane
y	y-direction
yy	y-plane
z	z-direction
zz	z-plane

Superscripts

.	Derivative
'	Division by flight velocity normalization

1. INTRODUCTION

1.1. Objective of the Present Work

Automated control is an essential element of flight. Flight properties such as altitude or velocity can be manipulated through electrical and mechanical means for the purpose of controlled flight. For some rocket designs and missions, attitude control is sufficient for accomplishing a flight objective.

With the apparent importance of control systems, the desire for a plan for control prescription was realized. With this realization, a plan for control prescription is desired. Therefore, the plan for the present work is to present a plan of control prescription. When a plan is established, an example is to be presented so that a reader would be capable of following. After presenting the example, system changes would be performed in order to also present examples of system refinement.

For the following work, it was assumed that a rocket with known qualities is in need of an effective means of control; in particular, a means of attitude control is desired for the rocket. The goal main goal of this example is to establish a system of attitude control for the given rocket. When the control system is established, refinements will be made in an attempt to improve the system's response.

1.2. Control System Design Approach

The formulated plan of attitude control system design has four main steps, the rocket design, the flight plan, the dynamics analysis, and the gain schedule. These design steps are summarized in Table 1.1.

Table 1.1: Control System Plan of Design

1. Rocket Design	2. Flight Plan	3. Dynamics Analysis	4. Gain Schedule
<ul style="list-style-type: none">• rocket properties are determined• control coefficients are determined• controlling electronics and mechanism properties are known	<ul style="list-style-type: none">• velocity schedule is prescribed• atmospheric conditions are determined	<ul style="list-style-type: none">• reference frames are established• dynamic equations are formulated• transfer functions are derived	<ul style="list-style-type: none">• the gain schedule is prescribed• system dynamic response is observed• adjustments and improvements are made

The rocket design step is the establishment of rocket information important to the dynamics of the system. The flight plan step is where expected atmospheric and flight conditions are established. The information from these steps are used as inputs for the dynamics analysis step, where the dynamic equations for the system are established and analyzed. The dynamics analysis is then used in the final step to prescribe a gain schedule, a table of control inputs to be used at discrete moments of the flight. In the final step, modifications to the flight plan and control system are performed until the system response becomes acceptable.

2. ROCKET DESIGN

Knowing the physical properties of the flight vehicle is needed to understand the dynamics of the vehicle. The rocket that is considered for control system design was considered to be a 7 foot tall, radially symmetric model rocket with the physical characteristics summarized in Table 2.1.

Table 2.1: Relevant Rocket Properties

Rocket Property	Value
Total Rocket Mass	1.1429 slugs
Fuel Mass	0.1415 slugs
Average Motor Thrust	247.4 lbf
Motor Burn Time	3.17 s
Drag Coefficient	0.518
Initial Static Margin	1.6
Final Static Margin	2.15
Initial I_{xx}	0.06056 slug ft ²
Final I_{xx}	0.05951 slug ft ²
Initial I_{yy}	10.66 slug ft ²
Final I_{yy}	10.50 slug ft ²
Initial I_{zz}	10.66 slug ft ²
Final I_{zz}	10.50 slug ft ²
Reference Area, S	0.307 ft ²

The total rocket mass is defined as the sum of all weights, motor and fuel included. The y-plane and z-plane moments of inertia are the same because the rocket is radially symmetric. The reference area is the body's circular cross-sectional area. The motor was assumed to be an Aerotech L1150R rocket motor, which has the average thrust and burn time shown. The properties in this table are used as inputs for the dynamics analysis.

The control coefficients relevant to the rocket and flight plan chosen are shown in Table 2.2.

TABLE 2.2: Relevant Rocket Coefficients

Coefficient	Per Radian Value
C_{lp}	-0.040
$C_{l\delta}$	0.173
C_{mq}	-11.56
$C_{m\alpha}$	0.460
$C_{m\dot{\alpha}}$	-0.100
$C_{m\delta}$	6.55
C_w	$-(m^*g)/(S^*q)$
$C_{z\alpha}$	-13.73
$C_{z\delta}$	-3.33

The coefficients shown in Table 2.2 are the nondimensional effectiveness of a property on the respective directional force or moment. For example, $C_{z\alpha}$ is the effectiveness of the attack angle on the total z-directional force. The relevant coefficients may vary depending on the formulated dynamic equations relevant to the system; for this reason, the relevant coefficients may be determined during the dynamics analysis. These coefficients are most often valued through analysis.

The rocket in consideration is assumed to use four servos that actuate control flaps, which provide an aerodynamic force for attitude control. The servos can deflect the flaps to a designed maximum of 10 degrees. The transfer function for a servo can be determined through experimentation if it is not provided by the manufacturer. This equation is used to add the servo's response dynamics to the system of control. The servos on the rocket is assumed to be well represented by the equation below.

$$\frac{\delta(s)}{e_a(s)} = \frac{1}{s^2 + 10s + 40}$$

The above equation is the continuous-time transfer function for the servo. If needed, a continuous-time transfer function can be expressed as a discrete-time transfer function using a zero-order hold (ZOH). Assuming a 0.1 second sampling time, a ZOH conversion of the servo's transfer function is shown below.

$$\frac{\delta(z)}{e_a(z)} = \frac{0.003566z + 0.00255}{z^2 - 1.123z + 0.3679}$$

3. FLIGHT PLAN

The flight plan is an intended flight path of the vehicle. The flight plan considered for this analysis is one intended to test the control system. From a vertical takeoff, the rocket would be commanded to perform a roll and pitch maneuver before reaching peak altitude. The roll maneuver would be prescribed to be a 90 degree angle change; it would be commanded at the moment of launch and it would be held throughout the flight. The pitch maneuver would be prescribed to be a 10 degree turn with a return to vertical flight. If these maneuvers are performed during a flight, angular and rate gyro data can be recorded and used to improve the control system through the comparison and analyzation of the recorded data. When the rocket reaches maximum altitude, a recovery chute would be deployed, so control is to be terminated at this point of the flight.

A yaw maneuver could be included in the flight plan, but the pitch and yaw dynamics are the same for a symmetric rocket, which was assumed for the rocket; this assumption is not always valid, so it needs to be verified for the vessel being considered. If the vessel is symmetric and all servos are operated during flight, a yawing maneuver would be redundant.

For the dynamic analysis, the aerodynamic conditions of the flight plan need to be determined. These conditions can be approximated through various means. With gravity and aerodynamic drag considered, the equations of motion could be integrated to approximate expected flight conditions at discrete flight times. Alternatively, a preliminary flight could be performed for the purpose of recording accelerometer and barometer data. However the flight conditions are approximated, they are imperative for the dynamic analysis step of control system design.

The flight conditions used for the analysis were approximated through the use of a MATLAB program that integrates the equations of motion using a fourth order Runge-Kutta integration. Assuming a vertical flight from takeoff to maximum altitude, the approximation suggests that the rocket will experience the flight conditions shown in Figure 3.1.

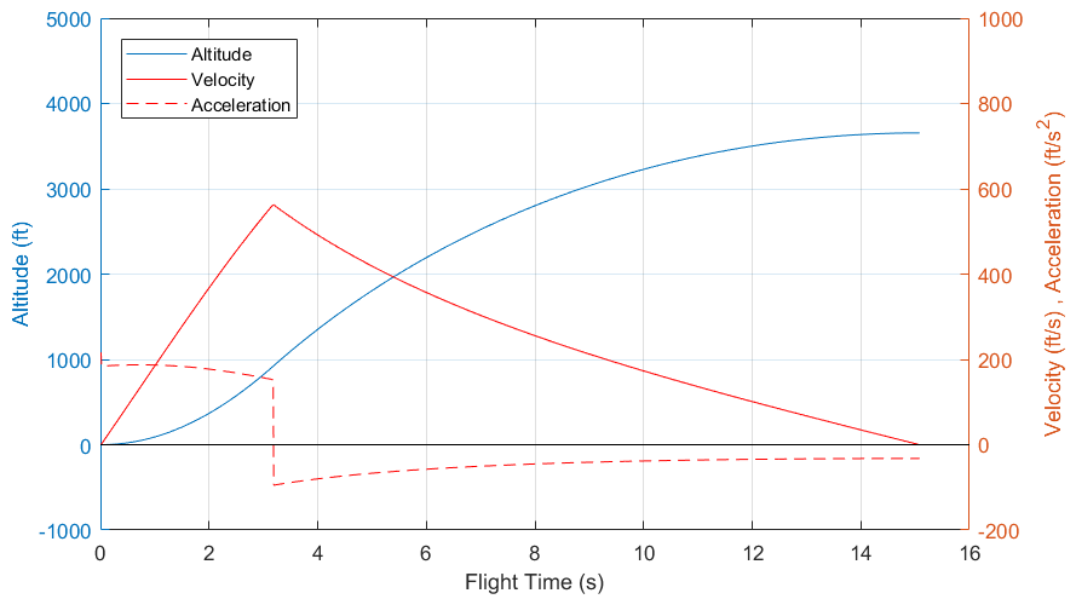


Figure 3.1: Expected Rocket Flight

For the simulated flight presented in the figure, air density and motor thrust was assumed constant. These are not reasonable assumptions to make for every flight; these assumptions need to be carefully considered for each flight. With the estimation performed, the rocket is expected to reach a maximum altitude of approximately 3600 feet, 15.1 seconds after launch. At this altitude, there is an approximate 10% reduction in atmospheric density, a change small enough to be ignored, so an assumed constant air density for the dynamics analysis step is assumed justified for this flight. With the assumption of constant motor thrust and fuel consumption, it is also expected that the rocket’s velocity will reach a maximum 560 feet per second. The mass and moments of inertia of the rocket are also expected to linearly change from the initial values to final values shown in Table 2.1. The assumption of constant thrust and fuel consumption again needs to be carefully considered for each individual vessel. With the chosen motor, this assumption is considered reasonable for the simulation performed.

With the simulation performed, the chosen flight plan at discrete times is shown in Table 3.1.

Table 3.1: Flight Plan at Discrete Times

time (s)	altitude (ft)	velocity (ft/s)	ϕ_{comm} (deg)	θ_{comm} (deg)
0.0	0.0	0.0	90	0
1.0	91.2	184.7	90	0
2.0	368.1	367.6	90	0
3.0	821.3	535.4	90	0
4.0	1351.9	491.8	90	0
5.0	1806.1	418.8	90	10
6.0	2193.2	356.9	90	10
7.0	2522.7	303.2	90	10
8.0	2801.7	255.6	90	10
9.0	3035.4	212.6	90	10
10.0	3228.0	173.0	90	0
11.0	3382.4	136.1	90	0
12.0	3500.9	101.1	90	0
13.0	3585.1	67.5	90	0
14.0	3636.2	34.8	90	0
15.0	3654.8	2.5	90	0

With this flight plan, the rocket could be prescribed 5 seconds to perform each maneuver. It needs to be verified by the dynamics analysis that this is enough time to perform the desired actions.

4. DYNAMICS ANALYSIS

The flight properties to be controlled, roll and pitch, need to be mathematically represented. The purpose of this is to model the dynamics of the system to assist in prescribing control gains. In order to mathematically model the dynamics, a set of coordinate systems needs to be established.

4.1. Coordinate Systems

In order to mathematically represent the rocket's roll and pitch, an established coordinate system between the rocket's frame of reference and a secondary frame of reference needs to be established. The secondary reference frame is usually centered somewhere on Earth, so it is commonly referred as the Earth frame, as it will be referred onwards. To establish the Earth frame for this analysis, the z-axis of the Earth frame will be considered the vertical direction, perpendicular to the horizontal plane; the x- and y-axes of the Earth frame are arbitrarily arranged East and North, respectively; and the origin of this frame is considered to be centered on the rocket CG at the moment of launch.

Depending on the flight plan, the relevant six equations of motion that govern a rocket will change. For example, a vessel on an orbital mission needs to account for the rotation of the Earth frame. Since the rocket being considered would not reach an altitude at which Earth's rotation is relevant, the Earth frame in this case was considered stationary and nonrotating.

The rocket reference frame and some relative angles are presented in Figure 4.1.

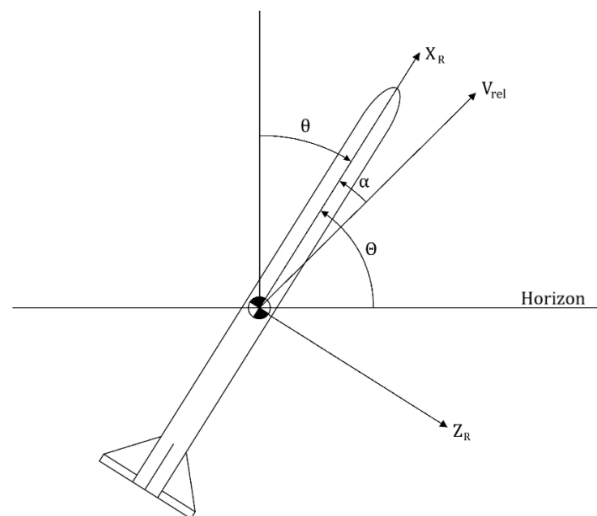


Figure 4.1: Rocket Frame and Relevant Angles

Shown in Figure 4.1, the rocket frame x-axis points from the rocket CG to the nose of the rocket. The y- and z-axes are each arranged parallel to one of the four orthogonally arranged control fins. At the moment of launch, the rocket frame's origin is considered centered on the Earth frame; the x-axis is arranged vertically; and the y- and z-axes are arbitrarily arranged East and North, respectively.

4.2. Equations of Motion

With an established coordinate system, the equations of motion can be formulated and manipulated for control. With the established properties and approximations, the general lateral Earth frame equations of motion can be expressed by the equations below:

$$C_{F_y} = -\frac{d}{2U} C_{y_p} \dot{\phi} - C_{y_\phi} \phi + \left(\frac{mU}{S\bar{q}} - \frac{d}{2U} C_{y_r} \right) \dot{\psi} - C_{y_\psi} \psi + \frac{mU}{S\bar{q}} \dot{\beta} - C_{y_\beta} \beta$$

$$C_l = \frac{I_{xx}}{S\bar{q}d} \ddot{\phi} - \frac{b}{2U} C_{l_p} \dot{\phi} - \frac{I_{xz}}{S\bar{q}d} \ddot{\psi} - \frac{d}{2U} C_{l_r} \dot{\psi} - C_{l_\beta} \beta$$

$$C_n = -\frac{I_{xz}}{S\bar{q}d} \ddot{\phi} - \frac{d}{2U} C_{n_p} \dot{\phi} + \frac{I_{zz}}{S\bar{q}d} \ddot{\psi} - \frac{d}{2U} C_{n_r} \dot{\psi} - C_{n_\beta} \beta$$

Additionally, the general longitudinal Earth frame equations of motion can be expressed as shown:

$$C_{F_x} = \left(\frac{mU}{S\bar{q}} \dot{u} - C_{x_u} u \right) + \left(-\frac{d}{2U} C_{x_\alpha} \dot{\alpha} - C_{x_\alpha} \alpha \right) + \left[-\frac{d}{2U} C_{x_q} \dot{\theta} - C_w \cos(\Theta) \theta \right]$$

$$C_{F_z} = (-C_{z_u} u) + \left[\left(\frac{mU}{S\bar{q}} - \frac{d}{2U} C_{z_\alpha} \right) \dot{\alpha} - C_{z_\alpha} \alpha \right] + \left[\left(-\frac{mU}{S\bar{q}} - \frac{d}{2U} C_{z_q} \right) \dot{\theta} - C_w \sin(\Theta) \theta \right]$$

$$C_m = (-C_{m_u} u) + \left(-\frac{d}{2U} C_{m_\alpha} \dot{\alpha} - C_{m_\alpha} \alpha \right) + \left(\frac{I_{yy}}{S\bar{q}d} \ddot{\theta} - \frac{d}{2U} C_{m_q} \dot{\theta} \right)$$

These equations were derived in detail by Blakelock¹ for general flight purposes. With simplifications and approximations, they can be applied to the given rocket and proposed flight plan. With some manipulation, they can be transformed into a usable form for analysis. The above equations are not applicable to all

rockets or flight plans. Rocket symmetry, Earth's rotation, and other factors may affect the form of these equations.

Particularly with airplanes and rockets, equation formulation is dependent on the established coordinate systems and angles. Depending on the source, some symbols may represent different quantities. In particular, the previously stated equations use the angles that are stated in Figure 4.2 below.

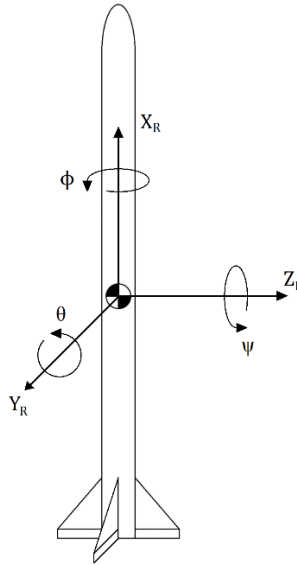


Figure 4.2: Rocket Axes and Angles of Attitude

In the figure, the rocket's axes are shown with their respective attitude angles. Phi is the roll angle, theta is the pitch angle, and psi is the yaw angle.

4.3. Roll Dynamics

Several choices of control systems exist; new systems of control can also be developed and chosen. For the given rocket and flight plan, the initial method of roll control was chosen to be a proportional negative feedback loop. This chosen control loop is displayed in Figure 4.2.

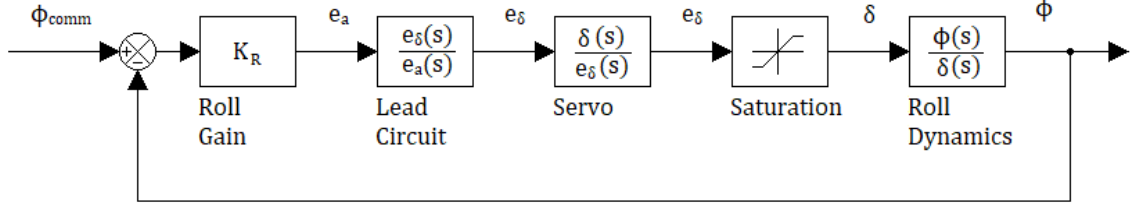


Figure 4.3: Roll Control Feedback Loop

In Figure 4.3, K_R is the roll control gain to be prescribed to the system. The servo block is the servo's contribution to the system. The roll dynamics block is the lateral dynamics' contribution to the system. The lead circuit is an additional block to be chosen for its effect on the system's stability. If needed, a lead circuit could be included to help stabilize the system. For this analysis, English units and radians were used for each block. Degrees were avoided for consistency and to prevent confusion. For system improvement, another system could be chosen when refining the system; but for now a proportional feedback control loop was observed.

Using the lateral dynamics equations, the roll dynamics transfer function can be derived. Because of the given rocket and expected flight plan, only the rolling moment equation is needed since the other equations contribute only minor effects to the rolling mode. The sideslip and yaw angles can also be neglected since they similarly contribute only minor effects. With the addition of a control force, a Laplace transform of the roll equation alters it as shown:

$$C_{l_{\delta_r}} \delta_r(s) = \left(\frac{I_{xx}}{S\bar{q}d} s^2 - \frac{d}{2U} C_{l_p} s \right) \phi(s)$$

Rearranged, the above equation provides the desired roll dynamics transfer function, shown below.

$$\frac{\phi(s)}{\delta(s)} = \frac{C_{l_{\delta_r}}}{\left(\frac{I_{xx}}{S\bar{q}d} s^2 - \frac{d}{2U} C_{l_p} s \right)}$$

4.4. Pitch Dynamics

As an initial system to test, it was decided that Pitch could be controlled by the same feedback loop system as the roll system, as shown in Figure 4.4.

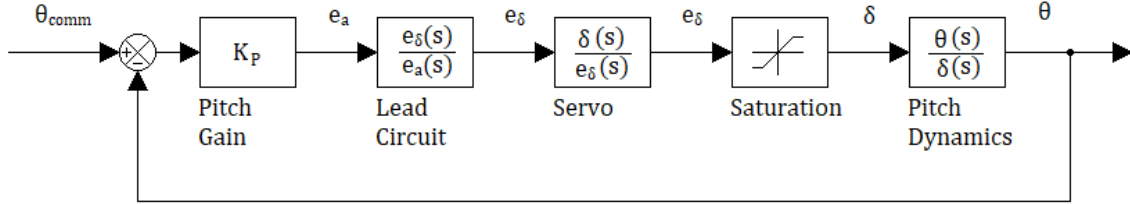


Figure 4.4: Pitch Control Feedback Loop

The blocks in the pitch control system are similar to the roll control system. Radians were again used for each block to prevent confusion. Depending on the dynamics of the system and the discretion of the user, the pitch system's lead circuit could be of different value and function to that of the roll system's lead circuit.

The pitch dynamics transfer function is formulated by taking the Laplace transform of the longitudinal state equations:

$$C_{x\delta}\delta(s) = \left(\frac{mU}{S\bar{q}}s - C_{x_u}\right)'u(s) + \left(-\frac{c}{2U}C_{x\dot{\alpha}}s - C_{x\alpha}\right)'\alpha(s) + \left[-\frac{c}{2U}C_{x_q}s - C_w \cos(\Theta)\right]\theta(s)$$

$$C_{z\delta}\delta(s) = (-C_{z_u})'u(s) + \left[\left(\frac{mU}{S\bar{q}} - \frac{c}{2U}C_{z\dot{\alpha}}\right)s - C_{z\alpha}\right]'\alpha(s) + \left[\left(-\frac{mU}{S\bar{q}} - \frac{c}{2U}C_{z_q}\right)s - C_w \sin(\Theta)\right]\theta(s)$$

$$C_{m\delta}\delta(s) = (-C_{m_u})'u(s) + \left(-\frac{c}{2U}C_{m\dot{\alpha}}s - C_{m\alpha}\right)'\alpha(s) + \left(\frac{I_{yy}}{S\bar{q}c}s^2 - \frac{c}{2U}C_{m_q}s\right)\theta(s)$$

Since the rocket would most likely encounter short-period oscillations, and since these are the most critical oscillations, these equations can be simplified by using a short-period approximation. At small angles of attack, the x-direction forces do not significantly contribute to longitudinal rotation, so the x-equation can be neglected. Short-period oscillations occur at constant velocity, so 'u is effectively zero. For specific missions or rockets, $C_{z\dot{\alpha}}$, C_{z_q} , and $C_{m\dot{\alpha}}$ can be disregarded because of their small contributions. For the given

rocket and flight plan, it is assumed that this is a reasonable assumption in this case. The equations as they pertain to the given rocket are then simplified further:

$$C_{z\delta}\delta(s) = \left(\frac{mU}{S\bar{q}}s - C_{z\alpha}\right)\alpha(s) + \left[-\frac{mU}{S\bar{q}}s - C_w \sin(\theta)\right]\theta(s)$$

$$C_{m\delta}\delta(s) = (-C_{m\alpha})\alpha(s) + \left(\frac{I_{yy}}{S\bar{q}c}s^2 - \frac{c}{2U}C_{m_q}s\right)\theta(s)$$

These simplifications are specific to the given rocket and flight plan, so these simplifications cannot always be made. But since they are applicable to the given rocket, the above equations can be rearranged to represent the pitch dynamics, $\theta(s)/\delta(s)$.

5. GAIN SCHEDULE DETERMINATION

The last step in this control system development process is choosing appropriate control gains. The gain values need to be chosen for discrete moments in the flight. This is done so that a gain that stabilizes the rocket at one moment during the flight doesn't destabilize the rocket at other moments. For conciseness, a specific moment in flight is observed to demonstrate gain selection. The moment chosen to be observed is 3 seconds into the flight. At this point, velocity is expected to be near its maximum.

5.1. Roll Control Gain Determination

At 3 seconds into the flight, the roll dynamics' continuous transfer function takes the following value:

$$\frac{\phi(s)}{\delta(s)} = \frac{0.573}{0.001913s^2 - 0.01338s}$$

In combination with the servo transfer function, the stability of the system can be observed through the locus plot, which is shown in Figure 5.1.

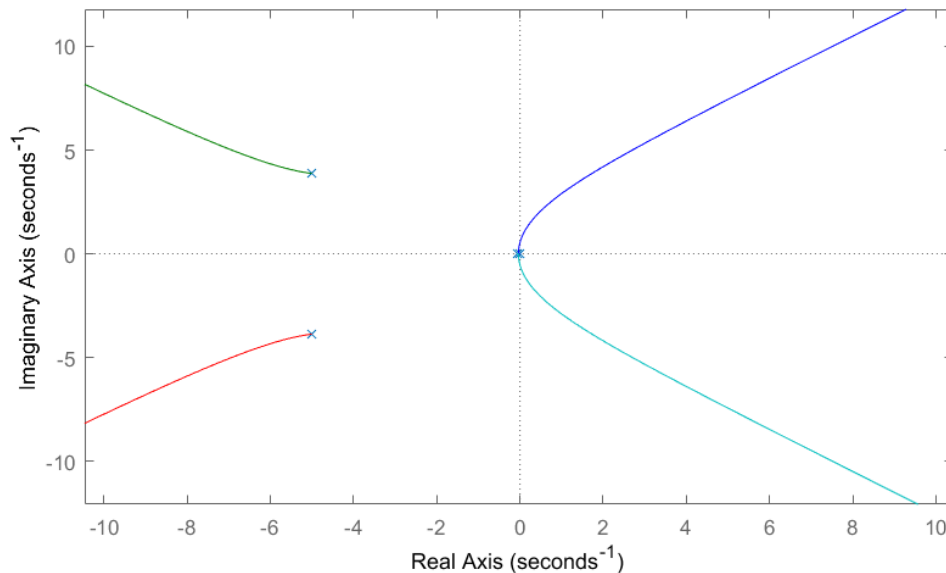


Figure 5.1: Root Locus Plot of Roll Dynamics, 3.0 Seconds into Flight

In the figure, there are two poles near the origin that cross into the right-half plane. Due to these poles, the system is unstable and thus requires a lead circuit for stabilization.

For stability, the lead circuit should have a zero near the origin to attract the destabilizing poles into the left-hand plane. The circuit also needs a pole to accompany the zero. Through trial and error, an initial lead circuit value was chosen, which is shown below:

$$\frac{e_{\delta}(s)}{e_{\phi}(s)} = \frac{4(s + 0.2)}{s + 10}$$

With a zero at -0.2 and a pole at -10, the lead circuit changes the locus plot as shown in Figure 5.2.

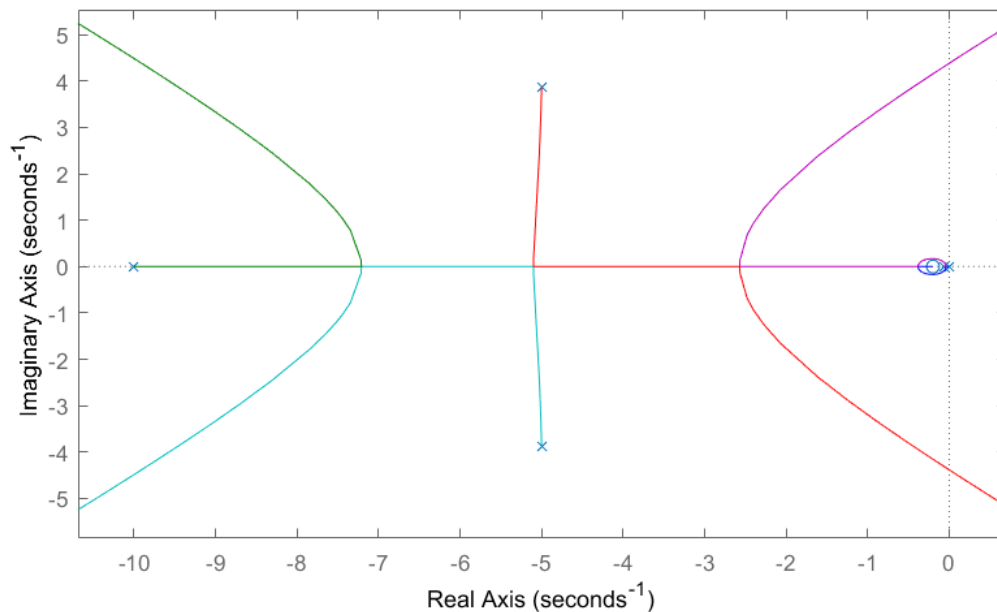


Figure 5.2: Root Locus Plot of Roll Dynamics with Lead Circuit

Shown in the figure, the destabilizing poles are attracted to the left-hand plane. At small gain values, this circuit stabilizes the system, allowing for control.

To observe the negative feedback response of the system, the system was modeled in Simulink by substituting the appropriate values and equations into the corresponding blocks in Figure 4.2. When a

90 degree step response is applied to the model with a 1.0 roll gain value, the system is expected to respond as shown in Figure 5.3.

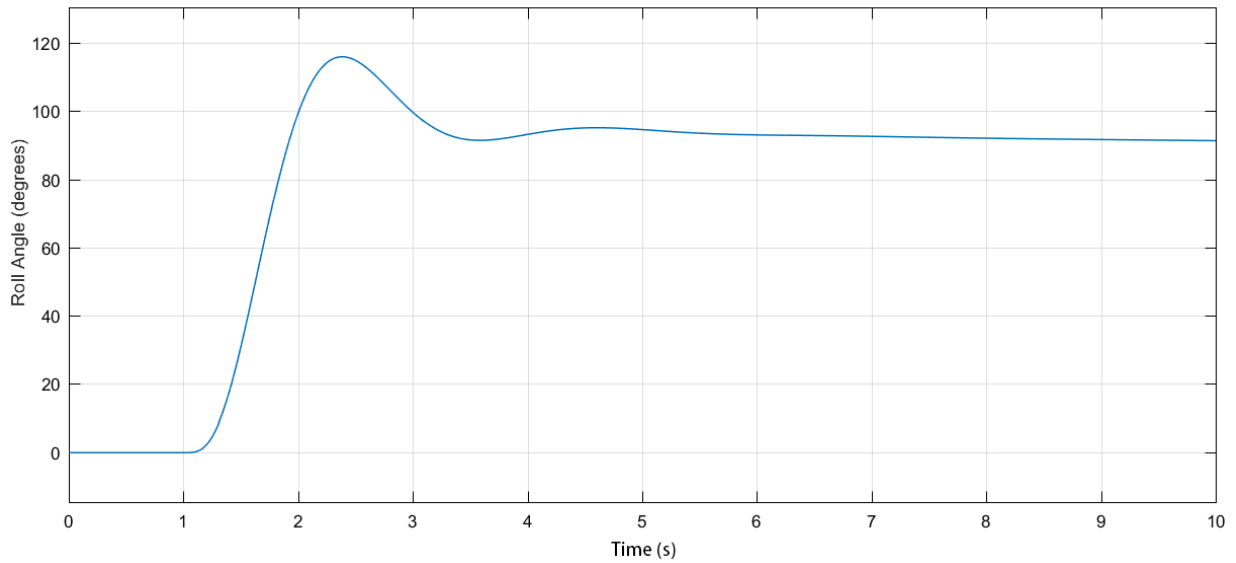


Figure 5.3: System Response to a 90 Degree Step Input

From the figure, the system is expected to initially overshoot the target roll angle before settling near the 90 degree target within 3 seconds after the step input. There is an error in the desired roll angle after 5 seconds, but it is assumed small enough to not be concerning.

The overshoot and settling qualities of the system's response can be modified by changing the roll gain. The system response with different gain values is shown in Figure 5.4.

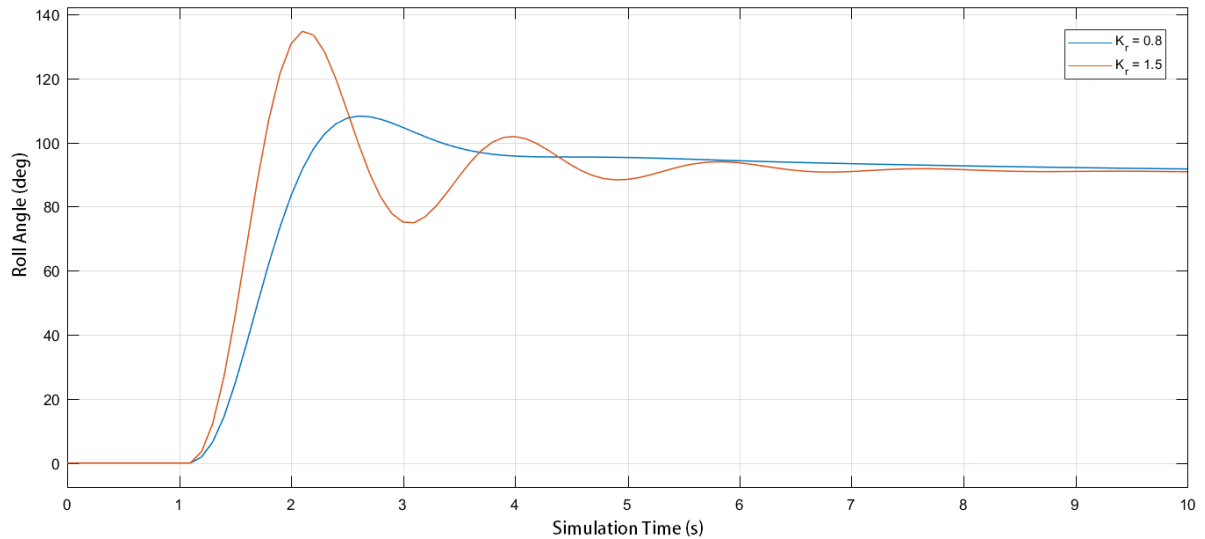


Figure 5.4: System Response with Various Gain Values

From the figure, it can be observed that the amount of overshoot is reduced at the cost of an increased settling time when the gain is reduced. The gain value can be increased in the pursuit of decreasing settling time, at the cost of increasing the overshoot amount; but with the system design chosen, an increase in gain value causes an increase in oscillation, increasing the settling time. After observing various gain values for this system, it was initially decided that a gain value of 1.0 has the most acceptable qualities of overshoot, settling time, and accuracy.

Since the dynamic analysis is an approximation of expected flight conditions, the actual flight conditions may vary. Because of this, it may benefit the analysis to observe varied flight conditions to determine the effect the chosen gain value may have on the system. Since air density isn't expected to vary significantly, it can be ignored. The flight velocity has a significant effect on the system, so the selected gain value needs to be observed at varying velocities. A 10% change in the expected velocity may provide a sufficient range of observation.

Three seconds into the flight, a 10% change in velocity has the upper and lower values of 588.9 ft/s and 481.9 ft/s. With the currently selected roll gain value, the system is expected to respond as shown in Figure 5.5.

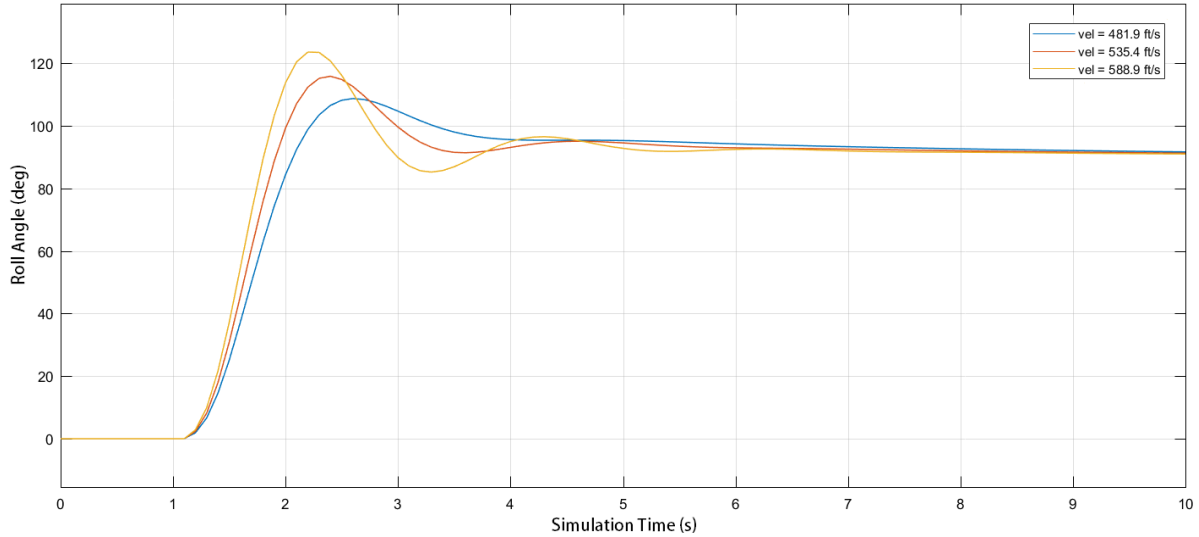


Figure 5.5: System Roll Response at Various Velocities

From the above figure, the settling time and roll angle error increases with a lower velocity. To avoid this, a new roll gain value of 1.2 was chosen since it would correct the undesired effect at lower velocities while still meeting the roll requirements at higher velocities.

If other flight qualities significantly affect the flight dynamics, such as air density or rocket mass, then changes in these qualities should also be observed to confirm the quality of the control system and selected gains. For the given rocket and flight plan, velocity is the main factor affecting the dynamics of this system. To select appropriate roll gain values for the entirety of the flight plan, the process outlined in this section was performed for each 0.5 second interval of the flight.

5.2. Pitch Control Gain Determination

The process for selecting pitch control gain values is the same as roll control gain selection. The pitch dynamics is also unstable with two poles entering the right-hand plane, which requires a lead circuit for stabilization. The lead circuit chosen for this system is shown in the equation below.

$$\frac{e_{\delta}(s)}{e_{\theta}(s)} = \frac{27(s + 0.4)}{s + 20}$$

With the servo, pitch dynamics, and the chosen lead circuit transfer functions, the root locus plot of the system is shown in Figure 5.6.

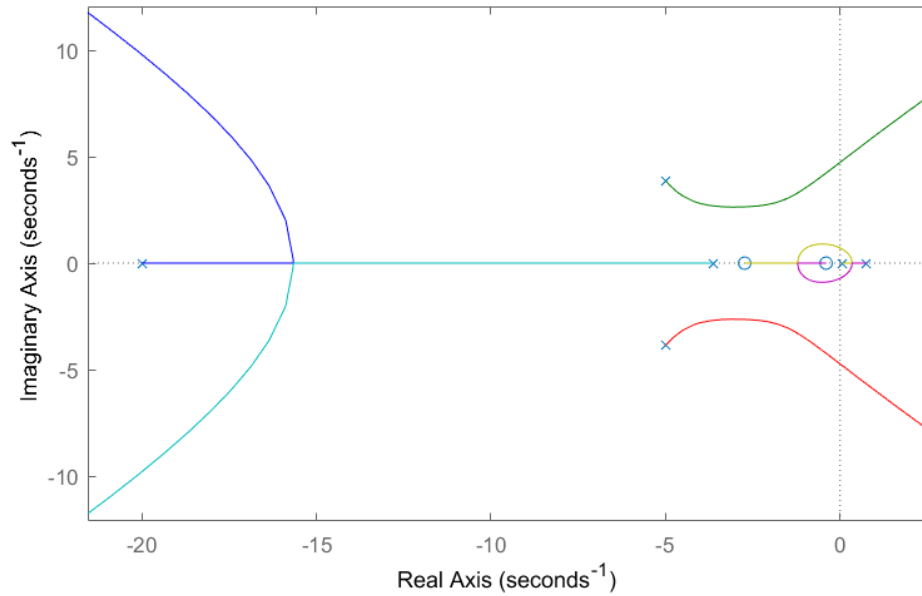


Figure 5.6: Root Locus Plot of Pitch Dynamics with Lead Circuit

Shown in the figure, the selected lead circuit attracts the two unstable poles into the left hand plane to stabilize the system, similar to the roll system lead circuit.

Like with the roll dynamics system, the pitch dynamics system was observed in Simulink to choose a stable gain value with desirable qualities. When this was performed, a gain value of 2.2 was selected for the system responses shown in Figure 5.7.

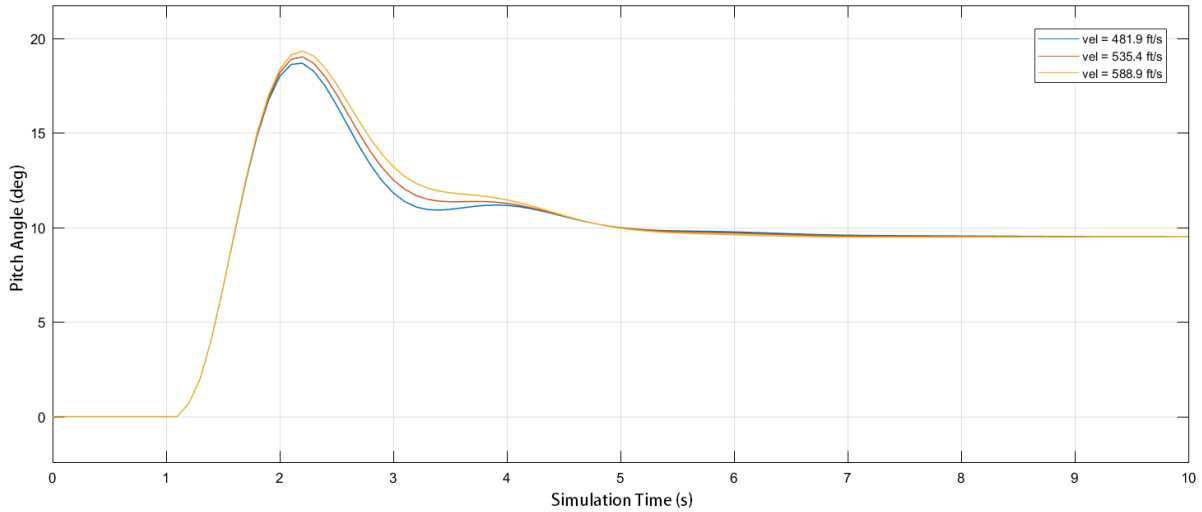


Figure 5.7: System Response at Various Velocities to a 10 Degree Step Input, $K_p = 2.2$

The figure shows that, with the chosen gain, there is an initial overshoot of the system before it settles to an approximate 9 degree pitch angle. This settling angle is in slight error of the desired 10 degrees, but it isn't extreme enough to be of concern. The figure also shows similar system responses with a 10% velocity change. Because of the qualities shown at the observed velocities, a pitching gain value of 2.2 was chosen for the given moment of flight. As with choosing roll control gains, this process is repeated for each 0.5 second interval of the expected flight.

6. Results and Discussion

The process outlined in section 5 was performed for all half-second intervals of the flight to choose an appropriate roll and pitch gain value for each moment. The initial gain values selected are shown in Table 6.1.

Table 6.1: Selected Control Gain Values

Flight Time (s)	Roll Gain	Pitch/Yaw Gain	Flight Time (s)	Roll Gain	Pitch/Yaw Gain
0.0	20.0	20.0	8.0	5.7	8.8
0.5	15.3	20.0	8.5	6.8	10.8
1.0	10.7	17.0	9.0	8.5	12.8
1.5	4.3	8.3	9.5	10.0	16.0
2.0	2.8	5.2	10.0	11.8	20.0
2.5	1.8	3.2	10.5	14.0	20.0
3.0	1.2	2.2	11.0	20.0	20.0
3.5	1.4	2.2	11.5	20.0	20.0
4.0	1.6	2.6	12.0	20.0	20.0
4.5	1.9	3.2	12.5	20.0	20.0
5.0	2.2	3.8	13.0	20.0	20.0
5.5	2.5	4.4	13.5	20.0	20.0
6.0	2.8	5.1	14.0	20.0	20.0
6.5	3.3	5.7	14.5	20.0	20.0
7.0	3.8	6.7	15.0	20.0	20.0
7.5	4.6	7.6			

Shown in the table, a higher gain value was chosen at times of lower velocity to increase the responsiveness of the system. To avoid outrageous gain value selection, a maximum gain value of 20 was set for the system. If needed, this maximum can be modified to meet the capabilities of the system installed in the rocket.

Since the refresh rate of the equipment is 0.1 seconds, a gain value can be chosen for each 0.1 second interval of the flight. Using the gain values in Table 6.1, the gain values not included in the table can be interpolated. A polynomial or spline interpolation would provide a smooth transition between the chosen gain values, but a linear interpolation could provide acceptable values for this system.

6.1. Initial Roll Control Results

It needs to be verified that the maneuvers can be performed in the given flight time. To verify the roll maneuver, a dynamic Simulink simulation was the tool chosen for this verification. This simulation was performed by updating and inputting the roll dynamics transfer function into the Simulink model and stepping the simulation through each 0.1 second interval. The result of the first 10 seconds of the simulation is shown in Figure 6.1.

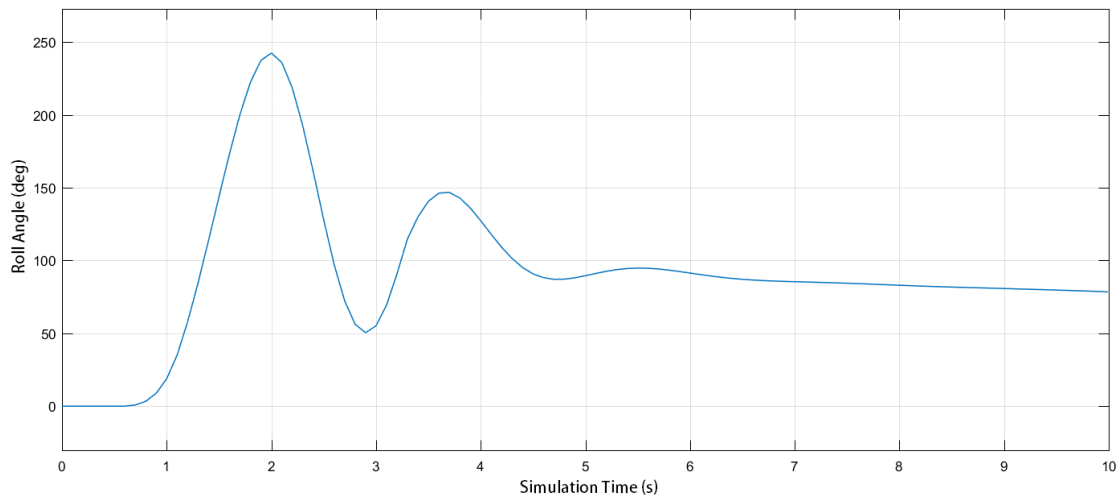


Figure 6.1: Simulink Roll Maneuver Simulation

Shown in Figure 6.1, the overshoot of the system is approximately 150 degrees beyond the target roll angle. This extreme overshoot causes a vibrational quality to the system that increases the settling time beyond an acceptable amount. In its current state, the system isn't expected to settle within the desired 5 second interval. Thus the current system of control is unable to achieve the flight plan. Modifications need to be made to improve the system.

Modifications that can be performed include choosing different gain values, modifying the flight plan, or choosing another feedback system. Modifying the rocket properties is possible in very specific cases, but it can be difficult if at all possible. It is also desired to avoid choosing another feedback system if possible. Since the present system response is attributed to the combination of the stepped roll command

and the high initial gain values, modifying these system qualities may help the system meet the desired flight plan.

6.2. Modifying Roll Gain Values to Improve System Response

Initially, different control gains for the first 3 seconds of flight were explored in an effort to correct the system response. Possible schemes that were explored include ramping gain values from zero until burnout and inputting a constant gain value until burnout. Other gain value schemes were explored, but for this system they produced similar results as to what is shown in Figure 6.2 below.

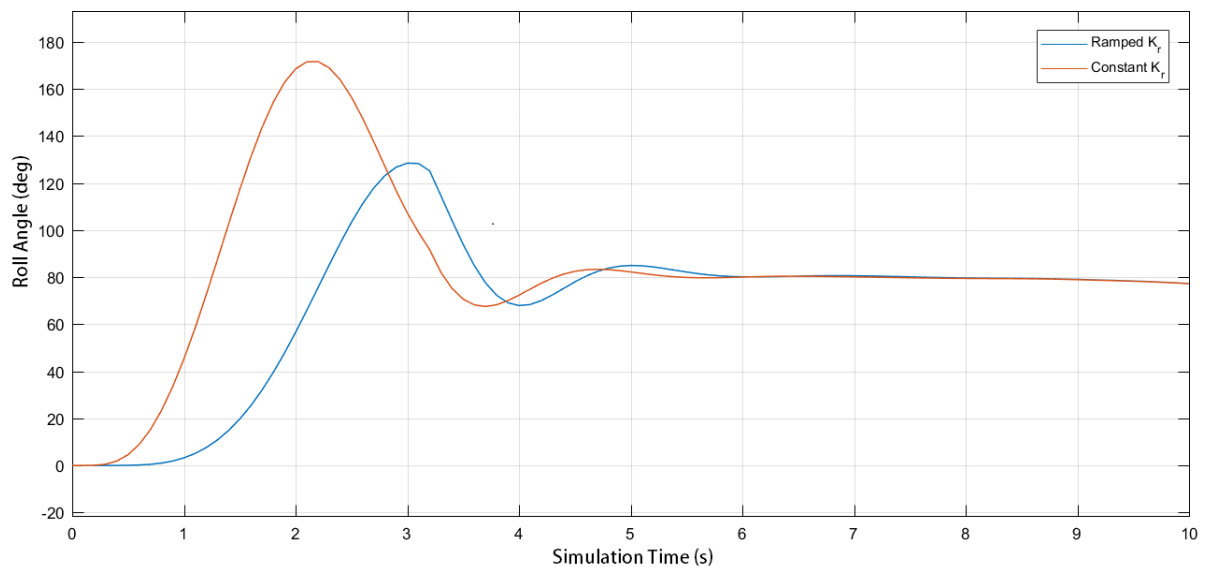


Figure 6.2: System Response to Modified Gain Schedules

In the figure, ramped and constant gain schedule schemes were simulated to determine the effect it would have on the system response. In both cases, the problem of overshoot is still present and causes settling issues for the system. For the constant gain value scheme, the approximate 80 degree overshoot is particularly undesirable. For the ramped gain value scheme, settling time is insufficient for the 5 second time interval. After observing multiple gain schedule schemes similar to these, it was determined that only modifying gain values would be insufficient for system response improvement.

6.3. Modifying the Roll Command to Improve System Response

When altering the gain values didn't produce a better system response, changes to the stepped rolling command were explored. Since the overshoot was in part attributed to the immediate 90 degree angle change command, an exploration of ramped angle command schemes may benefit the system response. To meet the 5 second time requirement, various ramped solutions were explored, which are shown in Figure 6.3.

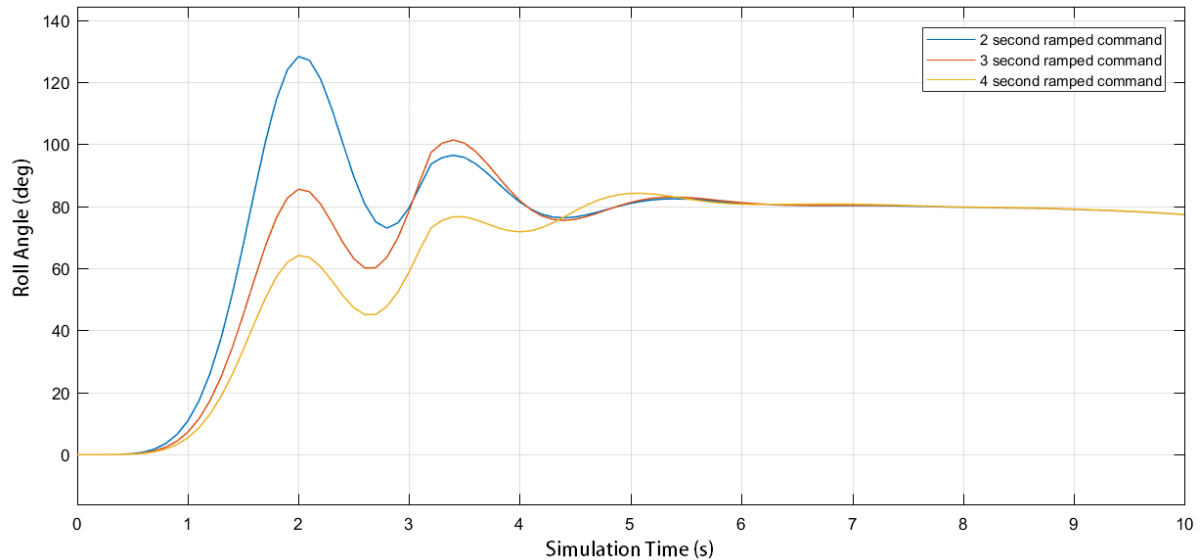


Figure 6.3: Ramped Command System Responses

The figure shows that each ramped roll command has a vibrational quality that isn't desirable. The vibrations dissipate with a lengthened ramping time, but with a desired 5 second settling time it isn't possible to completely dissipate the vibrations and settle the system within time. Each of the explored schemes in Figure 6.3 has an issue with settling time, none of them satisfyingly settle within the time limit.

On its own, a ramped command angle appears to not be the change needed to improve performance. Combined with an altered gain schedule, a satisfying solution could be possible. Still in pursuit of finding a satisfying system response without changing the chosen roll control system, various combinations of ramped commands and altered gain values were explored. A particular solution with a 3

second long ramped angle command and reduced gain values in the first second of launch was explored.

The simulation of this solution is shown in Figure 6.4.

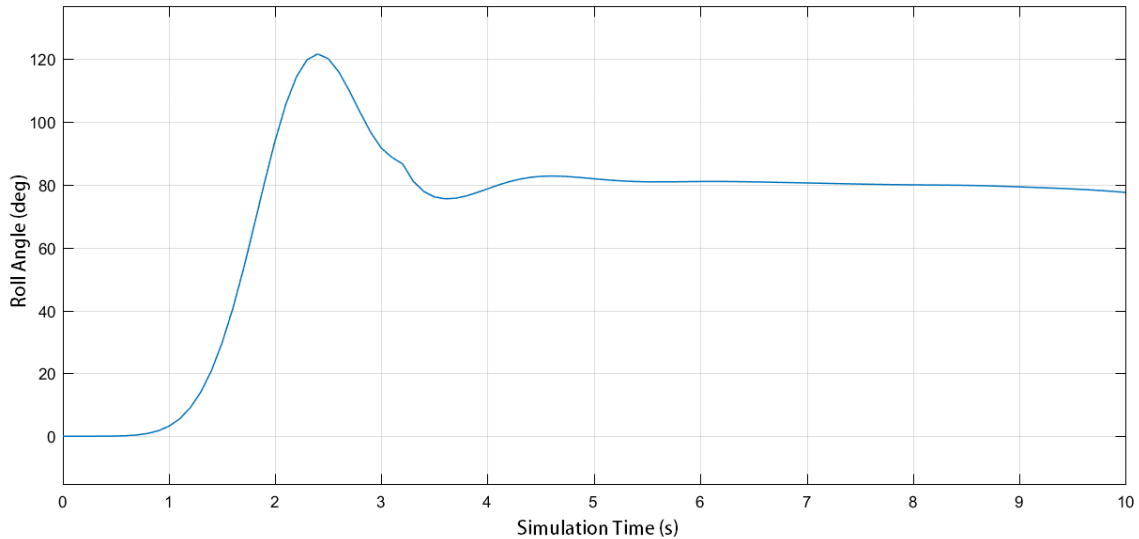


Figure 6.4: System Response to Gain Change and Ramped Command

In the figure, the system response has an approximate 30 degree overshoot, an 80% reduction from the original system response in Figure 6.1. With a gradual roll command, the vibrational quality of the system response was also reduced, resulting in a more satisfactory settling time. There is also an error of 10 degrees that arose from the changes; from the explored schemes previously displayed, this appears to be an effect inherent of the chosen system. If the system is chosen, this error needs to be considered if a launch is performed.

There is also a sharp change in roll angle at the moment of motor burnout. It is present in all the performed simulations, but it is especially noticeable in Figure 6.4. This sharp change was attributed to the dynamics of the system at burnout. The motor propulsion provided a roll dampening effect that was lost at burnout², which would account for this initially strange angle change.

6.4. Pitch Control Results

The pitch maneuvers need verification as well to ensure they can be performed in the given time. With the initially proposed flight plan and gain schedule, the same dynamic simulation method was applied to the pitching maneuvers, as shown in Figure 6.5.

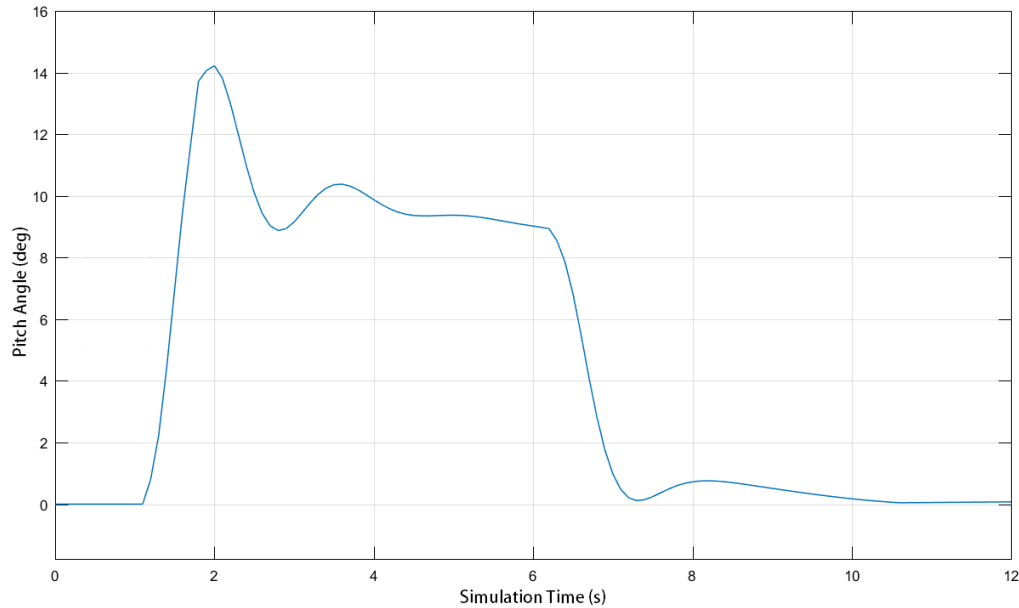


Figure 6.5: Simulink Pitch Maneuver Simulation

In the figure, the simulation was performed from 4 to 16 seconds into the flight. Five seconds into the flight, the rocket is commanded to a 10 degree pitch angle; the rocket is given 5 seconds to meet the commanded pitch angle before being commanded to return to a zero degree vertical flight, 10 seconds into the flight. From the simulation, it is expected that the rocket will meet both pitch angle commands within the allotted time, but with some error. The system response also has a 4 degree overshoot and vibrational quality, which was also present with the roll command. Although the system response is acceptable, it could be beneficial to explore ramped pitch commands.

As with the roll command, ramped pitch command options were explored in an effort to improve the system response. Without changing gain values, the pitch maneuvers were altered to be ramped over a 2 second period. A simulation of this alteration is shown in Figure 6.6.

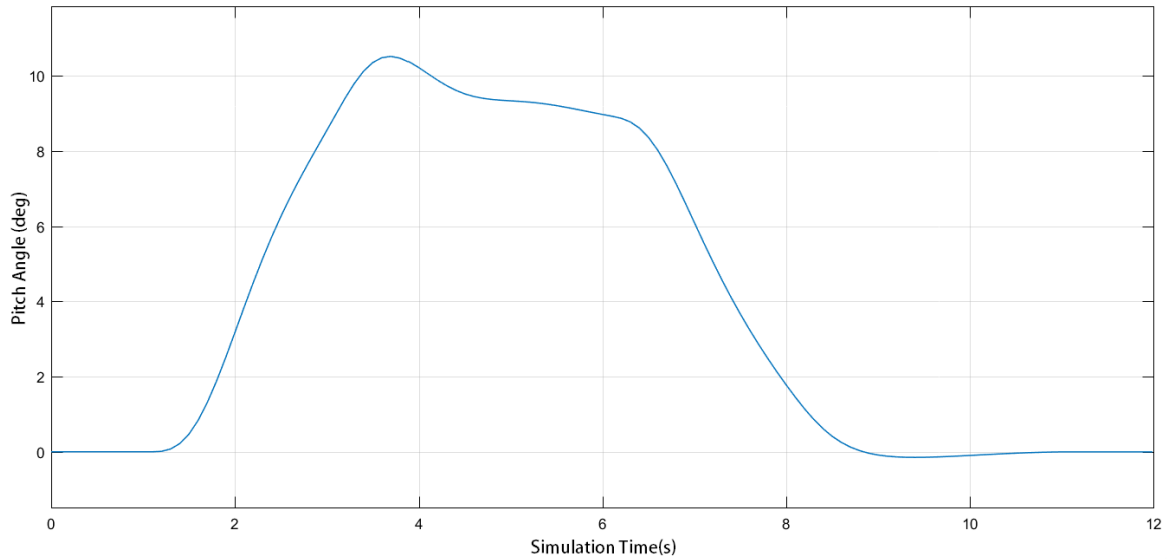


Figure 6.6: Ramped Pitch Maneuver Simulation

Shown in the figure, the overshoot and vibrational qualities of the initial pitch command were reduced by ramping the command angle. The return-to-zero command also has a reduced settling time. Although the error in command angle still exists, the ramped pitch maneuver is still considered an improvement on the stepped pitch maneuver.

7. CONCLUSIONS AND RECOMMENDATIONS

7.1. Conclusions of Study

The goal of the present work was to present a routine process of control system prescription. With a rocket of prescribed properties and flight plan, each step of the presented plan was followed until a system and gain values were chosen. When the simulated response was unsatisfactory, modifications were made to the control system and flight plan until an acceptable system response was simulated.

As shown in the results section, the initial flight plan and gain schedule benefits from the suggested modifications. The modified flight plan is summarized in the table below.

Table 7.1: Proposed Flight Plan

time (s)	altitude (ft)	velocity (ft/s)	ϕ_{comm} (deg)	θ_{comm} (deg)
0.0	0.0	0.0	0	0
1.0	91.2	184.7	30	0
2.0	368.1	367.6	60	0
3.0	821.3	535.4	90	0
4.0	1351.9	491.8	90	0
5.0	1806.1	418.8	90	0
6.0	2193.2	356.9	90	5
7.0	2522.7	303.2	90	10
8.0	2801.7	255.6	90	10
9.0	3035.4	212.6	90	10
10.0	3228.0	173.0	90	10
11.0	3382.4	136.1	90	5
12.0	3500.9	101.1	90	0
13.0	3585.1	67.5	90	0
14.0	3636.2	34.8	90	0
15.0	3654.8	2.5	90	0

In the table, the roll maneuver is suggested to be a 3 second long ramped command from 0 to 90 degrees, starting from launch and ending 3 seconds into the flight. Similarly, the pitch maneuvers are suggested to be 2 second long ramped commands to and from 10 degrees of pitch.

Similarly, the gain schedule appeared to benefit from a modification. From the simulation, the roll maneuver appeared to benefit from a reduction in gain value in the first second of flight. The final gain values that were decided upon are shown in Table 7.2.

Table 7.2: Proposed Gain Schedule

Flight Time (s)	Roll Gain	Pitch/Yaw Gain	Flight Time (s)	Roll Gain	Pitch/Yaw Gain
0.0	1.0	20.0	8.0	5.7	8.8
0.5	5.3	20.0	8.5	6.8	10.8
1.0	10.7	17.0	9.0	8.5	12.8
1.5	4.3	8.3	9.5	10.0	16.0
2.0	2.8	5.2	10.0	11.8	20.0
2.5	1.8	3.2	10.5	14.0	20.0
3.0	1.2	2.2	11.0	20.0	20.0
3.5	1.4	2.2	11.5	20.0	20.0
4.0	1.6	2.6	12.0	20.0	20.0
4.5	1.9	3.2	12.5	20.0	20.0
5.0	2.2	3.8	13.0	20.0	20.0
5.5	2.5	4.4	13.5	20.0	20.0
6.0	2.8	5.1	14.0	20.0	20.0
6.5	3.3	5.7	14.5	20.0	20.0
7.0	3.8	6.7	15.0	20.0	20.0
7.5	4.6	7.6			

With this gain schedule, the initial second of roll gains are reduced to avoid a possible extreme overshoot of the commanded roll angle. It may benefit the system to reduce the pitching gain values, but with no pitching maneuver until burnout, this may not be necessary. Otherwise, each gain value was chosen for its stable handling of the system at its respective flight velocity, while still being limited to a maximum value. The intermediate gain values can be chosen using interpolation; it was suggested that a linear interpolation would provide acceptable gain values.

7.2. Recommendations for Further Study

To help improve the analysis of the system, a test controlled flight is suggested. With a test flight, linear and rotational acceleration data can be recorded. The recorded data can be used to compare and improve upon the performed analysis.

Shown in Figure 6.1, there is some undesirable overshoot, command angle error, and vibrational qualities in the originally proposed control system. Most of these qualities were improved with the modifications proposed in tables 7.1 and 7.2. With the proposed modifications, it is expected that the rocket would meet the flight plan with a degree of error.

If a higher degree of flight control and accuracy is required, further modification would be necessary. Since the chosen control feedback loops were only proportional feedback systems, better control may be achievable with differential and integral feedback. This PID control solution would complicate the system by adding more control gains to be selected, but this PID system of control has been known to improve performance. This solution may be necessary for eliminating the steady-state error of the system's response.

Another possible solution for improving control is a system of nonlinear control. For the given rocket, aerodynamics through the use of control flaps is the driving control force, which is proportional to the square of relative flight velocity. It is expected that a nonlinear control system may provide more effective control. An exploration of the mentioned modifications is suggested for furthering the study of control.

8. REFERENCES

1. Blakelock, J.H., *Automatic Control of Aircraft and Missiles*, Second Edition, John Wiley & Sons, Inc., 1991.
2. Bengen, W.P., Caporaso, G.J., Mandell, G.K., *Topics in Advanced Model Rocketry*, The Massachusetts Institute of Technology, 1973.

APPENDICES

Appendix A - Vertical Flight MATLAB Simulation Program

```
%% RocketSim.m
% A Dynamics Simulator
% Randy Jones
% Last update: 2018-03-01
clear; close all; clc;

%% ENVIRONMENTAL VARIABLES
sim_time = 30; % simulation time , s
dt = 0.01; % time step , s
rho = .002377; % Air density , slug/ft^3
g = 32.2; % Acceleration due to gravity , ft/s^2

%% ROCKET DESIGN VARIABLES
mtot = 1.1429; % initial/total mass , slugs
mfuel = 0.1415; % fuel mass , slugs
Thrust = 247.4; % Ave Thrust from the motor , lbs
Ttime = 3.17; % Burn time of engine , s
CD = 0.518; % Drag coefficient
S = ((7.675/12)/2)^2*pi; % Reference area for drag force , ft^2

%% VECTOR CONSTRUCTION AND COMPLETION
t = dt:dt:sim_time; % Time vector
t = t';
T = ones(numel(t),1).*Thrust; % Constant thrust vector
m = linspace(mtot,mtot-mfuel,Ttime/dt)'; % Mass vector during burn

for n = floor(Ttime/dt)+1 : numel(t)
    T(n) = 0; % Completed thrust vector
    m(n) = mtot-mfuel; % Completed mass vector
end

%% STATE VECTOR INITIALIZATION
X = nan(numel(t),3); % Linear state vector each time step
X(1,:) = [0 0 T(1)/m(1)]; % Initial linear state vector

%% SIMULATION LOOP
for i = 2 : numel(t)
    X(i,:) = RK4_3D(X(i-1,:),dt,g,rho,m(i-1),S,CD,T(i-1));

    %% LOOP-END CHECK, ending program once condition is met
    % Current condition: Max altitude: velocity becomes negative
    if X(i,2) < 0
        X = X(1:i,:);
        t = t(1:i);
        m = m(1:i);
        T = T(1:i,:);
        break
    end
end
end
```

Appendix B - Fourth-Order Runge-Kutta Integrator for MATLAB

```
function [ X2 ] = RK4_3D( X0,dt,g,rho,m,S,CD,T )
% This program performs a Runge-Kutta-4 integration on a projectile in 3D
% cartesian space.
%
% X 2 = linear state vector of form [ pos,vel,accel ]

%% RUNGE-KUTTA INCREMENTS
k1 = projectile_ode(X0 ,g,rho,m,S,CD,T);
k2 = projectile_ode(X0 +dt.*k1./2,g,rho,m,S,CD,T);
k3 = projectile_ode(X0 +dt.*k2./2,g,rho,m,S,CD,T);
k4 = projectile_ode(X0 +dt.*k3 ,g,rho,m,S,CD,T);

%% NEXT ITERATION STATE VECTORS AND ATTITUDE
X2 = X0 + dt*(k1 + 2*k2 + 2*k3 + k4)/6;
X2(3) = (X2(2) - X0(2))/dt;

return
```

Appendix C - Rocket Vertical Flight State Equation Program for MATLAB

```
function [Xdot] = projectile_ode(X,g,rho,m,S,CD,T)
% PROJECTILE_ODE
% This file gives the ODEs for a projectile in motion. It uses Etkin's
% notation as seen in the book "Dynamics of Flight". It requires a
% unit quaternion to represent attitude.

qbar = .5*rho*X(2)^2; % Dynamic pressure
Da = qbar*(S)*(CD)/m; % Aerodynamic drag
Ta = T/m; % Motor acceleration

%% "Xdot" or "d(X)/dt"
Xdot = zeros(1,3);
Xdot(1) = X(2);
Xdot(2) = -g -Da +Ta;
Xdot(3) = 0;

return
```

Appendix D - Transfer Function Input Program for MATLAB and Simulink

```

%% TF_Determination.m
%
% This program is meant to be used in conjunction with NCSU_RocketSim.m
% to produce roll and pitch transfer functions, usable by Simulink for
% simulation.
% Sections for servo and lead network transfer function input and
% editing are available if needed.

%% INITIAL CONDITION VALUES

n = 300; % Time selection, assuming a 0.01 s time step
m = m(n); % rocket mass , slugs
d = 7.675/12; % reference length, rocket diameter , ft
U = X(n,6); % flight velocity , ft/s
qdyn = 0.5*rho*U^2; % dyn pressure , lb/ft^2

if n <= 317
    Ix = Iz(n); % MOI during motor burn , slug*ft^2
    Iy = Iy(n); % MOI during motor burn , slug*ft^2
else
    Ix = Iz(end); % MOI after motor burn , slug*ft^2
    Iy = Iy(end); % MOI after motor burn , slug*ft^2
end

%% CONTROL PROPERTIES AND IMPORTANT QUANTITIES
TH0 = 90; % initial pitch angle from horizon , deg
Cma = 0.46; % d(M)/d(alpha)
Cmad = -0.10; % d(M)/d(alpha-dot)
Cza = -13.73; % d(Fz)/d(alpha)
Czad = 0; % d(Fz)/d(alpha-dot)
Cmq = -11.56; % d(M)/d(q)
Cmdel = 6.55; % d(M)/d(delta) , (T*1)/(S*q*d)
Czdel = -3.33; % d(Fz)/d(delta) , -T/(Sq)
Cw = -m*g/(S*qdyn); % -(m*g)/(S*q) , -CL
Cldel = 0.173; % d(L)/d(delta)
Clp = -0.04; % d(L)/d(p)
Ts = 0.10; % sampling time , s

%% SERVO TF
servo_NUM = 1;
servo_DEN = [1 10 40];
servo_TFc = tf(servo_NUM,servo_DEN); % Servo continuous time TF
servo_TFd = c2d(servo_TFc,Ts); % Servo discrete time TF

%% ROLL TF
roll_NUM = [0 0 Cldel]; % Roll dynamics TF numerator
roll_DEN = [Ix/(S*qdyn*d) -d*Clp/(2*U) 0]; % Roll dynamics TF denominator

roll_zeros = roots(roll_NUM); % Zeros due to roll dynamics
roll_poles = roots(roll_DEN); % Poles due to roll dynamics
roll_TFc = tf(roll_NUM,roll_DEN); % Continuous time TF
roll_TFd = c2d(roll_TFc,Ts); % Discrete time TF

%% ROLL LEAD NETWORK TF
lead_r_zero = -0.2; % Roll lead network zero selection

```

```

lead_r_pole = -10.0; % Roll lead network pole selection

lead_r_NUM = 4.*[1 -lead_r_zero];
lead_r_DEN = [1 -lead_r_pole];
lead_r_TFc = tf(lead_r_NUM,lead_r_DEN); % Continuous time TF
lead_r_TFd = c2d(lead_r_TFc,Ts); % Discrete time TF

%% PITCH TF
pitch_NUM = zeros(1,4);
pitch_NUM(3) = d*Cmad*Czdel/(2*U) +m*U*Cmdel/(S*qdyn); % s^1 term
pitch_NUM(4) = Cma*Czdel-Cmdel*Cza; % s^0 term

pitch_DEN = zeros(1,4);
pitch_DEN(1) = m*U*Iy/(S^2*qdyn^2*d); % s^3 term
pitch_DEN(2) = -d*m*Cmad/(2*S*qdyn) ...
               -d*m*Cmq/(2*S*qdyn) -Cza*Iy/(S*qdyn*d); % s^2 term
pitch_DEN(3) = d*Cmq*Cza/(2*U) -d*Cmad*Cw*sind(TH0)/(2*U) ...
               -m*U*Cma/(S*qdyn); % s^1 term
pitch_DEN(4) = -Cma*Cw*sind(TH0); % s^0 term

pitch_zeros = roots(pitch_NUM); % Zeros due to pitch dynamics
pitch_poles = roots(pitch_DEN); % Poles due to pitch dynamics
pitch_TFc = tf(pitch_NUM,pitch_DEN); % Continuous time TF
pitch_TFd = c2d(pitch_TFc,Ts); % Discrete time TF

%% PITCH LEAD NETWORK TF
lead_p_zero = -.4; % Pitch lead network zero selection
lead_p_pole = -20; % Pitch lead network pole selection

lead_p_NUM = 27.*[1 -lead_p_zero];
lead_p_DEN = [1 -lead_p_pole];
lead_p_TFc = tf(lead_p_NUM,lead_p_DEN); % Continuous time TF
lead_p_TFd = c2d(lead_p_TFc,Ts); % Discrete time TF

%% GAIN SELECTION
%
% In this section, a schedule of gains for each 0.5 second interval is
% chosen. Using these values, intermediate 0.1 second interval values
% are linearly interpolated.
%
% nn is a variable that is used to choose a specific gain value based on
% the chosen simulation time.

Kr_i = [1.0 2.0 3.7 4.3 2.8 1.8 1.2 1.4 1.6 1.9 2.2 ...
        2.5 2.8 3.3 3.8 4.6 5.7 6.8 8.5 10.0 11.8 ...
        14.0 20.0 20.0 20.0 20.0 20.0 20.0 20.0 20.0 20.0];

Kp_i = [20.0 20.0 17.0 8.3 5.2 3.2 2.2 2.2 2.6 3.2 3.8 ...
        4.4 5.1 5.7 6.7 7.6 8.8 10.8 12.8 16.0 20.0 ...
        20.0 20.0 20.0 20.0 20.0 20.0 20.0 20.0 20.0 20.0];

% Linear interpolation of roll gain schedule
Kr = zeros(1,30*5);
for i = 1 : 30
    Kr(1+5*(i-1)) = Kr_i(i);
    Kr(2+5*(i-1)) = Kr_i(i) +(Kr_i(i+1)-Kr_i(i))*(1)/5;

```

```

    Kr(3+5*(i-1)) = Kr_i(i) + (Kr_i(i+1)-Kr_i(i))* (2)/5;
    Kr(4+5*(i-1)) = Kr_i(i) + (Kr_i(i+1)-Kr_i(i))* (3)/5;
    Kr(5+5*(i-1)) = Kr_i(i) + (Kr_i(i+1)-Kr_i(i))* (4)/5;
end

% Linear interpolation of roll gain schedule
Kp = zeros(1,30*5);
for i = 1 : 30
    Kp(1+5*(i-1)) = Kp_i(i);
    Kp(2+5*(i-1)) = Kp_i(i) + (Kp_i(i+1)-Kp_i(i))* (1)/5;
    Kp(3+5*(i-1)) = Kp_i(i) + (Kp_i(i+1)-Kp_i(i))* (2)/5;
    Kp(4+5*(i-1)) = Kp_i(i) + (Kp_i(i+1)-Kp_i(i))* (3)/5;
    Kp(5+5*(i-1)) = Kp_i(i) + (Kp_i(i+1)-Kp_i(i))* (4)/5;
end

nn = floor(n/Ts); % Sampling interval to choose gain from schedule
Kr_in = Kr(nn); % Kr to input into Simulink simulation
Kp_in = Kp(nn); % Kp to input into Simulink simulation

```